

# Capacitive DNA Detection Driven by Electronic Charge Fluctuations in a Graphene Nanopore

Gustavo T. Feliciano,<sup>1,2</sup> Carlos Sanz-Navarro,<sup>3</sup> Mauricio Domingues Coutinho-Neto,<sup>2</sup> Pablo Ordejón,<sup>3,4</sup> Ralph H. Scheicher,<sup>5,\*</sup> and Alexandre Reilya Rocha<sup>6,†</sup>

<sup>1</sup>Departamento de Físico Química, Instituto de Química, Universidade Estadual Paulista (UNESP), 14800-060 Araraquara, São Paulo, Brazil

<sup>2</sup>Centro de Ciências Naturais e Humanas, Universidade Federal do ABC, 09210-580 Santo André, São Paulo, Brazil

<sup>3</sup>ICN2-Institut Català de Nanociència i Nanotecnologia, Campus UAB, 08193 Barcelona, Spain

<sup>4</sup>CSIC-Consejo Superior de Investigaciones Científicas, ICN2 Building, 08193 Barcelona, Spain

<sup>5</sup>Department of Physics and Astronomy, Division of Materials Theory, Uppsala University, SE-751 20 Uppsala, Sweden

<sup>6</sup>Instituto de Física Teórica, Universidade Estadual Paulista (UNESP), 01140-070 São Paulo, São Paulo, Brazil

(Received 25 September 2014; revised manuscript received 22 December 2014; published 9 March 2015)

The advent of parallelized automated methods for rapid whole-genome analysis has led to an exponential drop in costs, thus greatly accelerating biomedical research and discovery. Third-generation sequencing techniques, which would utilize the characteristic electrical conductance of the four different nucleotides, could facilitate longer base read lengths and an even lower price per genome. In this work, we propose and apply a quantum-classical hybrid methodology to quantitatively determine the influence of the solvent on the dynamics of DNA and the resulting electron transport properties of a prototypic sequencing device utilizing a graphene nanopore through which the nucleic-acid chain is threaded. Our results show that charge fluctuations in the nucleotides are responsible for characteristic conductance modulations in this system, which can be regarded as a field-effect transistor tuned by the dynamic aqueous environment.

DOI: 10.1103/PhysRevApplied.3.034003

## I. INTRODUCTION

Nucleotides form the building blocks of DNA. The information encoded by their ordered arrangement in the nucleic-acid chain provides the set of instructions for all processes occurring in any living being on this planet. Thus, determination of the whole genome sequence is the key to a fundamental understanding of a wide range of biologically relevant issues, ranging from evolutionary developments to finding genetic predispositions for hereditary pathologies [1]. Although we have witnessed a dramatic decrease in the cost of genome sequencing over the past five years [2], this price development has recently shown signs of asymptotic convergence (to a value slightly above USD \$1,000 per genome [3]), mainly due to the expenses of chemical reagents required in the process. Thus, whole genome sequencing still remains too costly for widespread routine application in health care, delaying the onset of personalized or precision medicine [4].

An alternative approach for DNA sequencing, that holds the potential to be several orders of magnitude less expensive, is the possibility of using nanosized pores in biological [5–8] or solid-state [9–14] membranes as a sieve for DNA strands to pass through. During this translocation process one aims at identifying the different nucleotides

momentaneously residing within the pore. If the four base types (adenine, guanine, cytosine, and thymine) could be differentiated through a physical mechanism, then this approach would allow for rapid whole genome sequencing without the usual requirements of DNA amplification or labeling. The discrimination could be accomplished through a variety of techniques, for example, by measuring the subtle changes in ionic current through the pore due to characteristic blockage by the different bases [8,15,16]. Alternatively, it has been theoretically proposed [17] and later experimentally demonstrated [18–20] that one could differentiate between each nucleobase by measuring the transverse tunneling current across DNA in the pore. The fundamental idea here centers on the fact that each nucleotide has a different electronic structure and, more importantly, couples differently to the electrodes [21], which characteristically affects the electronic transport properties. Different signatures in the conductance of each base could thus provide the means for sequencing DNA [17,21,22].

Within the solid-state nanopore family, one material has recently gained considerable attention: graphene [23], an atomically thin membrane, which possesses a number of intriguing electrical and mechanical properties [24,25], in particular high conductivity. The almost negligible thickness of graphene holds the best chances for the desired single-base resolution in electrical DNA sequencing, for example, in a nanofabricated gap by monitoring the current flowing between the sharp edges of two semi-infinite

\*ralph.scheicher@physics.uu.se

†reilya@ift.unesp.br

sheets of graphene acting as transverse electrodes [26]. Experimentally, it was shown shortly after this proposal that it is indeed possible to drive DNA through a nanopore in graphene and detect its presence via changes in ionic current [27–29]. Very recently, it was experimentally achieved to detect the translocation of double-stranded DNA through a nanopore in a graphene nanoribbon simultaneously by the usual drops in the ionic current and also either peaks or dips in the transverse electric current passing through the graphene nanoribbon around the nanopore [30].

There have been a number of theoretical investigations on nanopores in graphene for the application of DNA sequencing [31–36]. Many of these studies have focused on the use of a graphene nanoribbon, where the edge states play a major role in the transport. Most importantly, a proper theoretical description has to take into consideration both dynamical and environmental effects [37] from the water molecules and the counterions. Although a few of these issues have been addressed in the past, mostly either model Hamiltonians or very specific configurations were used.

A number of important questions are thus left open. In particular, it remains unclear whether or not it is possible to differentiate between the four different nucleotides in the simplest-possible graphene nanopore configuration using transverse conductance measurements. In order to answer these questions, we present here a systematic study of the electronic transport properties of a single-stranded DNA molecule within a graphene nanopore in an arrangement similar to the experimental setup of Traversi *et al.* [30]. A

combination of density-functional theory coupled to hybrid classical methods is utilized by us to take into consideration the effects of the solvent [38,39] together with a Green's-function formalism to calculate the electronic transport. We find that, with a simple and robust arrangement, it is possible to discern between two families of nucleotides. We also find a different mechanism for conductance changes which are associated with a capacitive effect due to induced charge fluctuations at the edges of the nanopore induced by the presence of the different nucleotides.

## II. METHODOLOGY

The system studied by us comprises a square-shaped graphene sheet of dimensions  $4\text{ nm} \times 4\text{ nm}$  containing a nanopore. This system is created by selectively removing carbon atoms to form a hexagonal-shaped orifice, approximately 1.3 nm wide, enclosed by zigzag edges [Fig. 1(a)]. The size of the nanopore is chosen as a compromise between experimental fabrication feasibility [27,28] and consideration for the computational expenses of the simulations. Dangling bonds, created by the removal of carbon atoms, are saturated with hydrogen atoms. This atomistic graphene nanopore model is then completely immersed in water with counterions present. We simulated both the empty pore as well as the case when a four-base-long single-stranded DNA (ssDNA) molecule is present, threaded through the nanopore, containing all four nucleotides occurring in DNA [Fig. 1(b)]. Each nucleotide possesses one negative charge localized in its phosphate group.

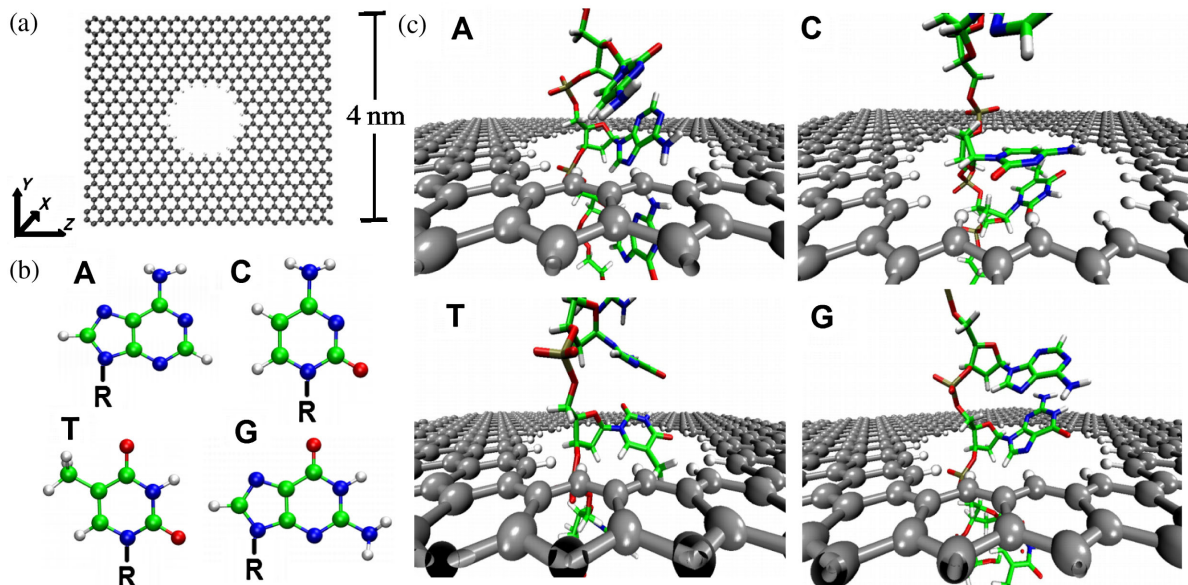


FIG. 1. (a) The schematic representation of the 1.3-nm-wide graphene nanopore model used in our simulations is shown. The transport occurs along the  $z$  direction. (b) The four nucleobases A, C, T, and G occurring in DNA are shown. Carbon atoms are shown in green, nitrogen in blue, oxygen in red, and hydrogen in white. R indicates the not-shown sugar-phosphate part that completes the nucleotide. (c) Typical snapshots from the molecular-dynamics simulations for each of the four nucleobase types located within the graphene nanopore are shown. For clarity, water molecules and counterions are removed from the image.

For our simulations, first, we sample the possible configurations of the DNA molecule and the solvent for each nucleobase type residing in the graphene nanopore using classical molecular-dynamics (MD) simulations. The system comprises a  $35 \text{ \AA} \times 40 \text{ \AA} \times 40 \text{ \AA}$  box containing 4400 water molecules and  $0.2M$  Na and Cl counterion concentration. An imbalance of four extra  $\text{Na}^+$  ions is introduced to compensate for the four negative charges from the phosphate groups of the ssDNA molecule, thus keeping the entire system neutral. The standard all-atom version of the AMBER99SB [40] empirical force field was used in the GROMACS [41] package to describe the interatomic potentials. We used the single-point-charge water model [42,43] and parameters for benzene to model graphene, with partial charges only in the hydrogen atoms terminating the nanopore edges and their neighboring carbon atoms.

We deliberately decided not to simulate here any actual translocation process of DNA through the pore, since any reasonably achievable simulation time is far from sufficient to approach a realistic speed of DNA during experiment. Rather, our aim is to sample over the fluctuations of a given nucleotide in the pore during the simulation time to maximize the statistical data obtained. As an initial configuration, each base is placed in the pore and a thermalization procedure is performed for 100 ps at 300 K using an *NVT* ensemble. We then equilibrate the water density for a further 200 ps using an *NPT* ensemble at 300 K and 1 bar with a Nose-Hoover thermostat and Parrinello-Rahman barostat. In both cases, we restrict the movement of the nucleotide inside the pore by preventing it from moving outside the pore, but allowing free movement within the plane of the graphene sheet. Finally, in the production stage, a 300-K *NVT* 3000-ps MD simulation is performed in which all the atoms are free to move. At this stage we allow the base to move, but apply a harmonic potential which prevents the base from adhering to graphene, as experimental results show that this effect clogs the nanopore [44].

From the resulting trajectories, 90 snapshots are randomly extracted from each passing nucleotide, spaced in time by approximately 100 ps (i.e., 100 000 1-fs time steps), which is enough to obtain uncorrelated snapshots for the “wobbling” effect of the base within the pore [45]. This procedure is repeated for three different initial configurations for each nucleobase in order to sample as much of the configuration space as possible. Typical snapshots obtained in our simulation are shown in Fig. 1(c), and all the sampled configurations are shown in Fig. S3 of the Supplemental Material [46].

To determine the electronic structure of the system under the external perturbation of the environment, the whole system is partitioned into a quantum-mechanical (QM) system, comprising the graphene sheet containing the nanopore and the passing nucleotide (between

645–648 atoms, depending on the nucleobase) and a molecular-mechanics (MM) system which includes all the water molecules, the counterions, and the nucleotides which are not, at a given instance, inside the pore [47,48]. This particular partitioning is tested considering one layer of water around each nucleobase treated quantum mechanically. The electronic transport properties, especially at the Fermi level, are essentially unchanged. The MM parameters from the AMBER99SB force field are again used [40]. The QM system is treated by first-principles calculations based on density-functional theory [49,50], using the generalized-gradient approximation for the exchange and correlation potential in its Perdew-Burke-Ernzerhof form [51]. Core electrons are replaced by norm-conserving pseudopotentials. The Kohn-Sham wave functions for the valence electrons are expanded in double- $\zeta$ -polarized basis sets for the nucleotide atoms and a double- $\zeta$  basis set for the graphene membrane. The calculations are carried out using the SIESTA code [52] with Brillouin zone sampling carried out only at the  $\Gamma$  point due to the size of the system. The MM potential is included as an external potential acting on the Kohn-Sham Hamiltonian. The atomic arrangement of a representative structure used in the QM calculations is shown in Fig. S2 where the electrostatic potential coming from the MM part is also shown [46].

Finally, once the Hamiltonian for each snapshot is obtained, we calculate the zero-bias transmission coefficients [53–55] using the nonequilibrium Green’s functions [56] as implemented in the SMEAGOL package [57,58]. The graphene sheet is attached to electrodes both to the left and to the right. In this work the electrodes are taken as pristine semi-infinite graphene. This setup represents an infinite graphene sheet containing the pore, an open system across which electrons will flow along the  $z$  direction (see Fig. 1). The building block of the semi-infinite electrode consists of a strip of 108 carbon atoms from the left and right sides of the graphene sheet containing the nanopore. Further details about our computational methods can be found in the Supplemental Material [46].

### III. RESULTS AND DISCUSSION

Figure 2(a) illustrates how much the conductance of the graphene nanopore changes when the dynamical environment of water and counterions is introduced into the system (but no DNA molecule yet). Specifically, we plot here the average difference in conductance between the pore with water molecules and counterions present and the empty (dry) pore. We note that, on the one hand, there are significant changes to the conductance for a wide range of energies, while on the other hand, at the Fermi level and for energies slightly below it, the average change and the standard deviation both tend to zero. In Fig. 2(b), we show the average total conductance of the pore with the four different nucleotides present (including solvent effects) and

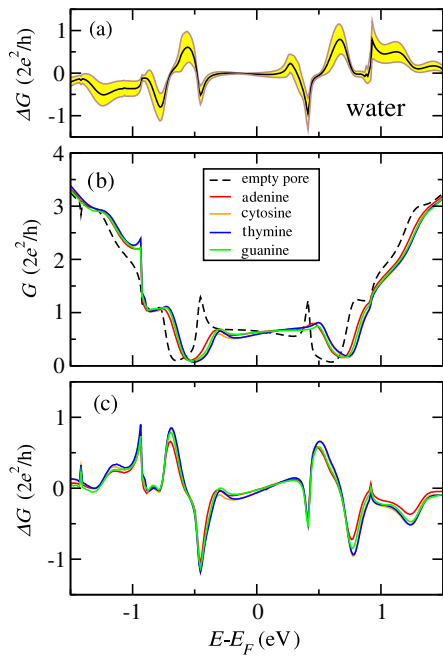


FIG. 2. (a) The black curve shows the average difference in conductance as a function of energy between the empty (dry) pore and the molecular-dynamics simulation of the pore containing water and counterions. The yellow area enveloping the black curve corresponds to  $\pm 1$  standard deviation from the mean. (b) Colored curves show the average conductance as a function of energy for each of the four DNA nucleotides when located in the pore with water and counterions present. The black dashed line shows the conductance of the empty (dry) pore as a reference. (c) The average difference in conductance is shown between the empty (dry) pore and the molecular-dynamics simulations of the four different nucleotides including the solvent and counterions.

compare it to the conductance of the empty (dry) pore as a reference. One notices that the curves for each of the DNA nucleobases are rather similar. This similarity is also observable in Fig. 2(c) where the average difference in conductance relative to the empty (dry) pore is plotted for the four different nucleotides.

It can be clearly seen that the presence of DNA affects conductance strongly. Overall, a shift can be observed, with prominent features of the conductance curve for the empty pore being shifted towards higher energies when DNA is present [Fig. 2(b)]. This shift is also observed when only solvent molecules are present, albeit to a smaller degree. Furthermore, relatively sharp features present in the curve for the empty pore, such as peaks near  $\pm 0.5$  eV and  $\pm 1$  eV, are suppressed when DNA is introduced to the pore [Fig. 2(b)]. These resonances can be associated with localized states similar to those expected to be present on the edges of graphene nanoribbons [59]. The more drastic changes can be seen most clearly in Fig. 2(c). Here, the suppression of peaks can be recognized as sharp peaks, while smoother shapes result for the shifts in areas where the conductance is relatively slowly changing as a function

of energy. This shift is mostly due to the fact that the nucleotides tend to become negatively charged. It thus creates an electric field which acts as a local gate on the graphene nanopore.

The difference in average conductance between the four DNA nucleotides is seen, from both panels (b) and (c) in Fig. 2, to be rather similar for most energies, thus not allowing one to easily distinguish between the four nucleotides based on the average value of conductance alone. However, the actual statistical distribution of conductance values does show some characteristic differences, in particular between the group of purine nucleobases guanine and adenine, and the pyrimidine nucleobases cytosine and thymine. Figure 3 shows the distribution of values of conductance change as a function of energy for each of the nucleotides. Albeit some differences can be observed, they are all qualitatively similar. When one focuses on the Fermi level, however, the differences become more noticeable.

In Fig. 4(a), therefore, we plot the conductance histogram for each of the four nucleotides at the Fermi energy  $E_F$ . Although small, clearly apparent differences are discernible between the two families of nucleobases, namely the purines (A and G) and the pyrimidines (C and T). The ratio between the peaks of the distributions of adenine and thymine, for example, is approximately 1.5, whereas for adenine and guanine, and thymine and cytosine, the difference is approximately 5% and 12%, respectively. However, the dynamical effects lead to a large broadening of the distributions, resulting in significant overlaps.

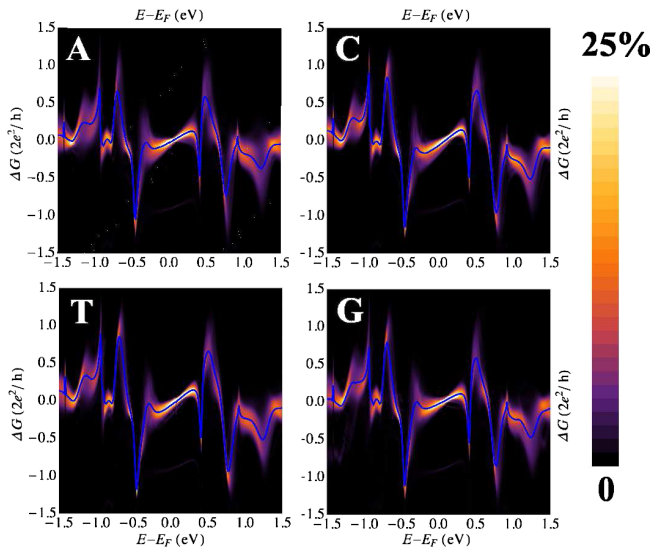


FIG. 3. Shown are the energy-resolved conductance distributions for the four different nucleotides in the graphene nanopore. Blue curves show the individual average conductance [superimposed plot in Fig. 2(c)], while the enveloping shaded areas (with the color gradient ranging from black over violet, orange, yellow, to white) indicates the percentage with which deviations from the average occur in the conductance at different energies for the four nucleotides.

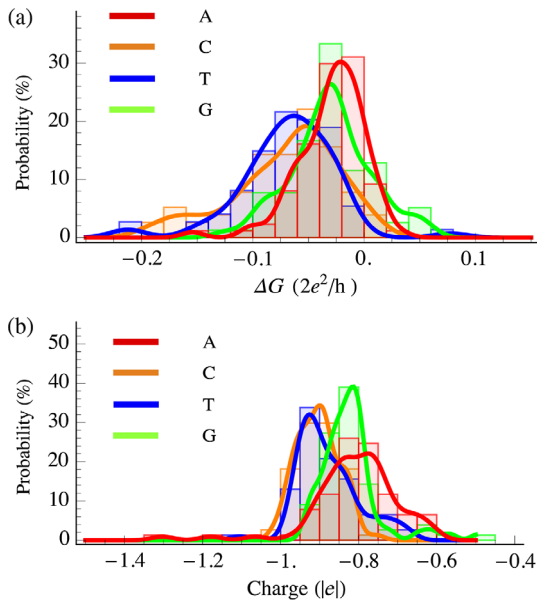


FIG. 4. (a) Distribution of the difference in conductance at the Fermi level from the empty (dry) pore case for the four different nucleotides in the graphene nanopore, presented as histogram bars and fitted distribution curves (this plot is thus a combined cross section of the data in Fig. 3 at  $E = E_F$ ). (b) Charge distribution in the nucleotides presented as histogram bars and fitted distribution curves.

Our findings do, however, enable us to highlight a different sensing mechanism for detecting DNA nucleotides in a graphene nanopore. In most works, tunneling across a gap has been considered. From our calculations it is clear that the nucleotides tend to be negatively charged. The charge carried by a nucleotide creates an electric field that changes the local chemical potential around the pore in a way similar to the working mechanism of a field-effect transistor. As we allow the molecule to move freely inside the pore, there are small charge fluctuations due to the interaction with the graphene sheet, which in turn influence the conduction. This behavior is evidenced by the histogram of the net charge on each of the nucleotides, presented in Fig. 4(b). We can clearly see a one-to-one correspondence between the distributions of fluctuating charges and the changes in conductance plotted in Fig. 4(a). The purines, comprising two aromatic rings, are seen to exhibit stronger interaction with the graphene sheet than the smaller pyrimidines with their single aromatic ring. Water here plays an important role, not only in the dynamics of the system, but also for stabilizing the net charge on each nucleobase, as it has been observed in a number of biological systems [60].

#### IV. CONCLUSIONS

In the present work, we utilize an electronic transport QM-MM approach to evaluate the feasibility of graphene nanopores as an all-electrical sequencing device for DNA,

taking into account the structural fluctuations of the nucleotides and the combined noise due to the rapidly altering electrostatic potentials of the solvent, the counterions, and the DNA molecule itself. The developed method considerably reduces the computational effort and at the same time captures the essential effects of the environment. The results show that the conductance difference between the nucleotides is considerably affected by the dynamics of the nucleobases within the pore. We also note that water is of fundamental importance in stabilizing the charged system.

We show that the fluctuations of the charge in a given nucleotide lead to an analogous distribution in the conductance change of the graphene nanopore system induced by the same nucleotide. In essence, the charging of the base leads to an effective electric field in the graphene sheet which influences the conductance. This effect could not be captured by model Hamiltonians, which are not self-consistently calculated for each configuration. The resulting capacitive transport mechanism can help explain experimental results for pores which are significantly larger than the nucleotides and would thus be extremely difficult to assess electronically through tunneling conductance.

Our findings lead us to conclude that all four nucleobase types will show similar conductances and that it would be hard to electrically distinguish between them in a graphene nanopore setup. Nonetheless, some degree of differentiation between the nucleobases appears to be possible. It is also important to note that the conducting pathways around the graphene nanopore yield larger transmission coefficients compared to those based on a tunneling current alone (e.g., in a nanogap). This effect could help to overcome the problem of noise in such devices. Finally, given the results of this work, functionalization of the atoms in the pore edge could significantly enhance nucleobase-pore interaction, thus reducing the structural noise by enhancing the graphene-nucleobase electronic coupling [32,61]. At the same time, functionalization could be tailored to achieve base-specific charge transfer. Hydroxide and amine groups are good candidates for functionalization. Hydroxide is expected to interact strongly with the nucleobases [62], due to the variety of possible interactions (it has a positive and a negative center of charge, plus the possibility for hydrogen bonding). Nitrogen (in the amine form) would also be a good candidate [34], with two centers of negative charge and one center of positive charge, and they both resemble the groups already present in complementary nucleobases in double-stranded DNA. In view of these results, it seems that, although the sources of noise remain, engineering functionalized graphene nanopores might still yield better strategies for the development of electrical DNA sequencing devices.

#### ACKNOWLEDGMENTS

The authors would like to thank S. Sanvito for valuable discussions. We also acknowledge financial support from

the São Paulo Research Foundation (FAPESP-Brazil, Grant No. 13/02112-0), CAPES-Brazil, Universidade Federal do ABC, CNPq, the Swedish Foundation for International Cooperation in Research and Higher Education (STINT), and the Swedish Research Council (VR, Grant No. 621-2009-3628). C. S. N. and P. O. were supported by Spanish MINECO through Grant No. FIS2012 37549 C05 (with joint financing by FEDER Funds from the European Union), and by the Severo Ochoa Program, Grant No. SEV-2013-0295. C. S.-N. acknowledges support from MINECO through the Ramon y Cajal Program.

[1] Francis S. Collins, Eric D. Green, Alan E. Guttmacher, and Mark S. Guyer, A vision for the future of genomics research, *Nature (London)* **422**, 835 (2003).

[2] Elaine R. Mardis, A decade's perspective on DNA sequencing technology, *Nature (London)* **470**, 198 (2011).

[3] K. A. Wetterstrand, DNA Sequencing Costs: Data from the NHGRI Genome Sequencing Program (GSP), <http://www.genome.gov/sequencingcosts/>.

[4] B. S. Shastray, Pharmacogenetics and the concept of individualized medicine, *Pharmacogenomics J.* **6**, 16 (2006).

[5] J. J. Kasianowicz, E. Brandin, D. Branton, and D. W. Deamer, Characterization of individual polynucleotide molecules using a membrane channel, *Proc. Natl. Acad. Sci. U.S.A.* **93**, 13770 (1996).

[6] D. W. Deamer and M. Akeson, Nanopores and nucleic acids: Prospects for ultrarapid sequencing, *Trends Biotechnol.* **18**, 147 (2000).

[7] Gerald M. Cherf, Kate R. Lieberman, Hytham Rashid, Christopher E. Lam, Kevin Karplus, and Mark Akeson, Automated forward and reverse ratcheting of DNA in a nanopore at 5-Å precision, *Nat. Biotechnol.* **30**, 344 (2012).

[8] Elizabeth A. Manrao, Ian M. Derrington, Andrew H. Laszlo, Kyle W. Langford, Matthew K. Hopper, Nathaniel Gillgren, Mikhail Pavlenok, Michael Niederweis, and Jens H. Gundlach, Reading DNA at single-nucleotide resolution with a mutant MspA nanopore and phi29 DNA polymerase, *Nat. Biotechnol.* **30**, 349 (2012).

[9] J. Li, D. Stein, C. McMullan, D. Branton, M. J. Aziz, and J. A. Golovchenko, Ion-beam sculpting at nanometre length scales, *Nature (London)* **412**, 166 (2001).

[10] A. J. Storm, J. H. Chen, X. S. Ling, H. W. Zandbergen, and C. Dekker, Fabrication of solid-state nanopores with single-nanometre precision, *Nat. Mater.* **2**, 537 (2003).

[11] Daniel Folopea, Marc Gershon, Bradley Ledden, David S. McNabb, Jene A. Golovchenko, and Jiali Li, Detecting single stranded DNA with a solid state nanopore, *Nano Lett.* **5**, 1905 (2005).

[12] Cees Dekker, Solid-state nanopores, *Nat. Nanotechnol.* **2**, 209 (2007).

[13] Bala Murali Venkatesan, David Estrada, Shouvik Banerjee, Xiaozhong Jin, Vincent E. Dorgan, Myung-Ho Bae, Narayana R. Aluru, Eric Pop, and Rashid Bashir, Stacked graphene-Al<sub>2</sub>O<sub>3</sub> nanopore sensors for sensitive detection of DNA and DNA-protein complexes, *ACS Nano* **6**, 441 (2012).

[14] Axel Fanget, Floriano Traversi, Sergey Khlybov, Pierre Granjon, Arnaud Magrez, László Forró, and Aleksandra Radenovic, Nanopore integrated nanogaps for DNA detection, *Nano Lett.* **14**, 244 (2014).

[15] Chaitanya Sathe, Xueqing Zou, Jean-Pierre Leburton, and Klaus Schulten, Computational investigation of DNA detection using graphene nanopores, *ACS Nano* **5**, 8842 (2011).

[16] Ping Xie, Qihua Xiong, Ying Fang, Quan Qing, and Charles M. Lieber, Local electrical potential detection of DNA by nanowire nanopore sensors, *Nat. Nanotechnol.* **7**, 119 (2011).

[17] Michael Zwolak and Massimiliano Di Ventra, Electronic signature of DNA nucleotides via transverse transport, *Nano Lett.* **5**, 421 (2005).

[18] Makusu Tsutsui, Masateru Taniguchi, Kazumichi Yokota, and Tomoji Kawai, Identifying single nucleotides by tunnelling current, *Nat. Nanotechnol.* **5**, 286 (2010).

[19] Shuai Chang, Shuo Huang, Jin He, Feng Liang, Peiming Zhang, Shengqing Li, Xiang Chen, Otto Sankey, and Stuart Lindsay, Electronic signatures of all four DNA nucleosides in a tunneling gap, *Nano Lett.* **10**, 1070 (2010).

[20] Aleksandar P. Ivanov, Emanuele Instuli, Catriona M. McGilvery, Geoff Baldwin, David W. McComb, Tim Albrecht, and Joshua B. Edel, DNA tunneling detector embedded in a nanopore, *Nano Lett.* **11**, 279 (2011).

[21] Michael Zwolak and Massimiliano Di Ventra, Physical approaches to DNA sequencing and detection, *Rev. Mod. Phys.* **80**, 141 (2008).

[22] Haiying He, Ralph H. Scheicher, Ravindra Pandey, Alexandre Reily Rocha, Stefano Sanvito, Anton Grigoriev, Rajeev Ahuja, and Shashi P Karna, Functionalized nanopore-embedded electrodes for rapid DNA sequencing, *J. Phys. Chem. C* **112**, 3456 (2008).

[23] K. S. Novoselov, A. K. Geim, S. V. Morozov, D. Jiang, Y. Zhang, S. V. Dubonos, I. V. Grigorieva, and A. A. Firsov, Electric field effect in atomically thin carbon films, *Science* **306**, 666 (2004).

[24] A. K. Geim and K. S. Novoselov, The rise of graphene, *Nat. Mater.* **6**, 183 (2007).

[25] A. H. Castro-Neto, F. Guinea, N. M. R. Peres, K. S. Novoselov, and A. K. Geim, The electronic properties of graphene, *Rev. Mod. Phys.* **81**, 109 (2009).

[26] Henk W. Ch. Postma, Rapid sequencing of individual DNA molecules in graphene nanogaps, *Nano Lett.* **10**, 420 (2010).

[27] Christopher A. Merchant, Ken Healy, Meni Wanunu, Vishva Ray, Neil Peterman, John Bartel, Michael D. Fischbein, Kimberly Venta, Zhengtang Luo, A. T. Charlie Johnson, and Marija Drndić, DNA translocation through graphene nanopores, *Nano Lett.* **10**, 2915 (2010).

[28] Grégory F. Schneider, Stefan W. Kowalczyk, Victor E. Calado, Grégory Pandraud, Henny W. Zandbergen, Lieven M. K. Vandersypen, and Cees Dekker, DNA translocation through graphene nanopores, *Nano Lett.* **10**, 3163 (2010).

[29] S. Garaj, W. Hubbard, A. Reina, J. Kong, D. Branton, and J. A. Golovchenko, Graphene as a subnanometre trans-electrode membrane, *Nature (London)* **467**, 190 (2010).

[30] F. Traversi, C. Raillon, S. M. Benameur, K. Liu, S. Khlybov, M. Tosun, D. Krasnozhon, A. Kis, and A. Radenovic, Detecting the translocation of DNA through a nanopore using graphene nanoribbons, *Nat. Nanotechnol.* **8**, 939 (2013).

[31] Tammie Nelson, Bo Zhang, and Oleg V. Prezhdo, Detection of nucleic acids with graphene nanopores: Ab initio characterization of a novel sequencing device., *Nano Lett.* **10**, 3237 (2010).

[32] Yuhui He, Ralph H. Scheicher, Anton Grigoriev, Rajeev Ahuja, Shubing Long, ZongLiang Huo, and Ming Liu, Enhanced DNA sequencing performance through edge-hydrogenation of graphene electrodes, *Adv. Funct. Mater.* **21**, 2674 (2011).

[33] Jariyanee Prasongkit, Anton Grigoriev, Biswarup Pathak, Rajeev Ahuja, and Ralph H. Scheicher, Transverse conductance of DNA nucleotides in a graphene nanogap from first principles, *Nano Lett.* **11**, 1941 (2011).

[34] Kamal K. Saha, Marija Drndić, and Branislav K. Nikolić, DNA base-specific modulation of microampere transverse edge currents through a metallic graphene nanoribbon with a nanopore, *Nano Lett.* **12**, 50 (2012).

[35] Stanislav M. Avdoshenko, Daijiro Nozaki, Claudia Gomes da Rocha, Jhon W. González, Myeong H. Lee, Rafael Gutierrez, and Gianaurelio Cuniberti, Dynamic and electronic transport properties of DNA translocation through graphene nanopores, *Nano Lett.* **13**, 1969 (2013).

[36] Ralph H. Scheicher, Anton Grigoriev, and Rajeev Ahuja, DNA sequencing with nanopores from an ab initio perspective, *J. Mater. Sci.* **47**, 7439 (2012).

[37] Johan Lagerqvist, Michael Zwolak, and Massimiliano Di Ventra, Influence of the environment and probes on rapid DNA sequencing via transverse electronic transport, *Biophys. J.* **93**, 2384 (2007).

[38] A. Warshel and M. Levitt, Theoretical studies of enzymic reactions: Dielectric, electrostatic and steric stabilization of the carbonium ion in the reaction of lysozyme, *J. Mol. Biol.* **103**, 227 (1976).

[39] Carlos F. Sanz-Navarro, Rogeli Grima, Alberto García, Edgar A. Bea, Alejandro Soba, José M. Cela, and Pablo Ordejón, An efficient implementation of a QM-MM method in SIESTA, *Theor. Chem. Acc.* **128**, 825 (2011).

[40] Viktor Hornak, Robert Abel, Asim Okur, Bentley Strockbine, Adrian Roitberg, and Carlos Simmerling, Comparison of multiple amber force fields and development of improved protein backbone parameters, *Proteins Struct. Funct. Bioinf.* **65**, 712 (2006).

[41] H. J. C. Berendsen, D. van der Spoel, and R. van Drunen, GROMACS: A message-passing parallel molecular dynamics implementation, *Comput. Phys. Commun.* **91**, 43 (1995).

[42] H. J. C. Berendsen, J. P. M. Postma, W. F. Gunsteren, and J. Hermans, Interaction models for water in relation to protein hydration, in *Intermolecular Forces: Proceedings of the Jerusalem Symposia on Quantum Chemistry and Biochemistry*, edited by Bernard Pullman (Springer, Netherlands, 1981), Vol. 14, pp. 331–342.

[43] H. J. C. Berendsen, J. R. Grigera, and T. P. Straatsma, The missing term in effective pair potentials, *J. Phys. Chem.* **91**, 6269 (1987).

[44] Grégory F. Schneider, Qiang Xu, Susanne Hage, Stephanie Luik, Johannes N. H. Spoor, Sairam Malladi, Henny Zandbergen, and Cees Dekker, Tailoring the hydrophobicity of graphene for its use as nanopores for DNA translocation, *Nat. Commun.* **4**, 2619 (2013).

[45] D. Genest, How long does DNA keep the memory of its conformation? A time-dependent canonical correlation analysis of molecular dynamics simulation, *Biopolymers* **38**, 389 (1996).

[46] See Supplemental Material at <http://link.aps.org/supplemental/10.1103/PhysRevApplied.3.034003> for an in-depth description of the methodology and transmission results considering no water molecules, and one layer of water described quantum mechanically.

[47] D. R. Lide, *Handbook of Chemistry and Physics*, 81st ed. (CRC Press, Boca Raton, FL, 2000).

[48] W. Wang, O. Donini, C. M. Reyes, and P. A. Kollman, Biomolecular simulations: Recent developments in force fields, simulations of enzyme catalysis, protein-ligand, protein-protein, and protein-nucleic acid noncovalent interactions, *Annu. Rev. Biophys. Biomol. Struct.* **30**, 211 (2001).

[49] P. Hohenberg and W. Kohn, Inhomogeneous electron gas, *Phys. Rev.* **136**, B864 (1964).

[50] W. Kohn and L. J. Sham, Self-consistent equations including exchange and correlation effects, *Phys. Rev.* **140**, A1133 (1965).

[51] John P. Perdew, Kieron Burke, and Matthias Ernzerhof, Generalized Gradient Approximation Made Simple, *Phys. Rev. Lett.* **77**, 3865 (1996).

[52] J. M. Soler, E. Artacho, J. D. Gale, A. García, J. Junquera, P. Ordejón, and D. Sánchez-Portal, The SIESTA method for *ab initio* order-*N* materials simulation, *J. Phys. Condens. Matter* **14**, 2745 (2002).

[53] R. Landauer, Spatial variation of currents and fields due to localized scatterers in metallic conduction, *IBM J. Res. Dev.* **1**, 223 (1957).

[54] M. Büttiker, Y. Imry, R. Landauer, and S. Pinhas, Generalized many-channel conductance formula with application to small rings, *Phys. Rev. B* **31**, 6207 (1985).

[55] R. Landauer, Conductance from transmission: Common sense points, *Phys. Scr.* **T42**, 110 (1992).

[56] S. Datta, *Electronic Transport in Mesoscopic Systems*, 1st ed. (Cambridge University Press, Cambridge, 1995).

[57] A. R. Rocha, V. M. García-Suárez, S. W. Bailey, C. J. Lambert, J. Ferrer, and S. Sanvito, Towards molecular spintronics, *Nat. Mater.* **4**, 335 (2005).

[58] A. R. Rocha, V. M. García-Suárez, S. Bailey, C. Lambert, J. Ferrer, and S. Sanvito, Spin and molecular electronics in atomically generated orbital landscapes, *Phys. Rev. B* **73**, 085414 (2006).

[59] Kyoko Nakada, Mitsutaka Fujita, Gene Dresselhaus, and Mildred S. Dresselhaus, Edge state in graphene ribbons: Nanometer size effect and edge shape dependence, *Phys. Rev. B* **54**, 17954 (1996).

[60] Moshe Faraggi and Federico Broitman, One-electron oxidation reactions of some purine and pyrimidine bases in aqueous solutions. Electrochemical and pulse radiolysis studies, *J. Phys. Chem.* **100**, 14751 (1996).

[61] Slaven Garaj, Song Liu, Jene A. Golovchenko, and Daniel Branton, Molecule-hugging graphene nanopores, *Proc. Natl. Acad. Sci. U.S.A.* **110**, 12192 (2013).

[62] Heejeong Jeong, Han Seul Kim, Sung-Hoon Lee, Dongho Lee, Yong Hoon Kim, and Nam Huh, Quantum interference in DNA bases probed by graphene nanoribbons, *Appl. Phys. Lett.* **103**, 023701 (2013).